

Handheld Point-of-Care System for Rapid Detection of SARS-CoV-2 Extracted RNA in under 20 min

Jesus Rodriguez-Manzano,* Kenny Malpartida-Cardenas, Nicolas Moser, Ivana Pennisi, Matthew Cavuto, Luca Miglietta, Ahmad Moniri, Rebecca Penn, Giovanni Satta, Paul Randell, Frances Davies, Frances Bolt, Wendy Barclay, Alison Holmes, and Pantelis Georgiou



Cite This: <https://dx.doi.org/10.1021/acscentsci.0c01288>



Read Online

ACCESS |



Metrics & More

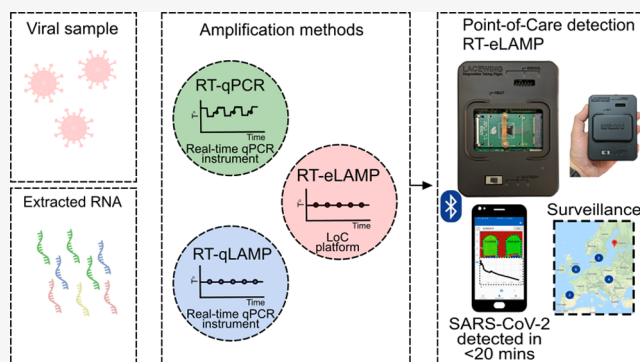


Article Recommendations



Supporting Information

ABSTRACT: The COVID-19 pandemic is a global health emergency characterized by the high rate of transmission and ongoing increase of cases globally. Rapid point-of-care (PoC) diagnostics to detect the causative virus, SARS-CoV-2, are urgently needed to identify and isolate patients, contain its spread and guide clinical management. In this work, we report the development of a rapid PoC diagnostic test (<20 min) based on reverse transcriptase loop-mediated isothermal amplification (RT-LAMP) and semiconductor technology for the detection of SARS-CoV-2 from extracted RNA samples. The developed LAMP assay was tested on a real-time benchtop instrument (RT-qLAMP) showing a lower limit of detection of 10 RNA copies per reaction. It was validated against extracted RNA from 183 clinical samples including 127 positive samples (screened by the CDC RT-qPCR assay). Results showed 91% sensitivity and 100% specificity when compared to RT-qPCR and average positive detection times of 15.45 ± 4.43 min. For validating the incorporation of the RT-LAMP assay onto our PoC platform (RT-eLAMP), a subset of samples was tested ($n = 52$), showing average detection times of 12.68 ± 2.56 min for positive samples ($n = 34$), demonstrating a comparable performance to a benchtop commercial instrument. Paired with a smartphone for results visualization and geolocalization, this portable diagnostic platform with secure cloud connectivity will enable real-time case identification and epidemiological surveillance.



INTRODUCTION

A novel coronavirus first identified in Wuhan (China) in December 2019 resulted in the implementation of stringent measures such as quarantine or air traffic closure as an effort to limit its spread. Declared as a pandemic by the World Health Organization (WHO), SARS-CoV-2 has spread globally with over 79.5 million cases and 1.76 million deaths worldwide.¹ The ability to accurately and reliably diagnose SARS-CoV-2, causing COVID-19 disease, is crucial for containing the pandemic enabling a proper response at national and global scales.

This highly contagious virus belongs to the genus of *Betacoronavirus* of the Coronaviridae family.^{2,3} As with all the human coronaviruses (hCoVs) identified to date, SARS-CoV-2 also has zoonotic origins.⁴ According to the WHO, the most common symptoms of this lower respiratory tract infection include fever, cough, fatigue, and pneumonia which can severely develop into acute respiratory distress syndrome and hyperinflammation.⁵ SARS-CoV-2 is characterized by presenting high transmissibility (mainly through aerosolized droplets from the saliva or nose), high infectivity, and a long incubation period (from 0 to 14 days).^{2,5} In particular, the high number of

asymptomatic subjects (mainly children and young adults) might be one of the major contributions to the rapid spread of this disease. Although several vaccine candidates have started to be distributed in the community, and antiviral treatments are in clinical trials,^{6–8} rapid diagnostics are critical to respond to the pandemic and reduce the spread of COVID-19.^{2,9} Notably, rapid and point-of-care (PoC) diagnostics are essential to expand, scale up, and increase the accessibility of testing around the world.

Different methods have been proposed for the diagnosis of SARS-CoV-2 including antigen detection, serologic tests, computerized tomography imaging, and nucleic acid amplification tests (NAATs).^{10,11} Serologic and antigen-based detection tests diagnose past and active infections, respectively; however, they commonly provide qualitative results and suffer

Received: September 23, 2020

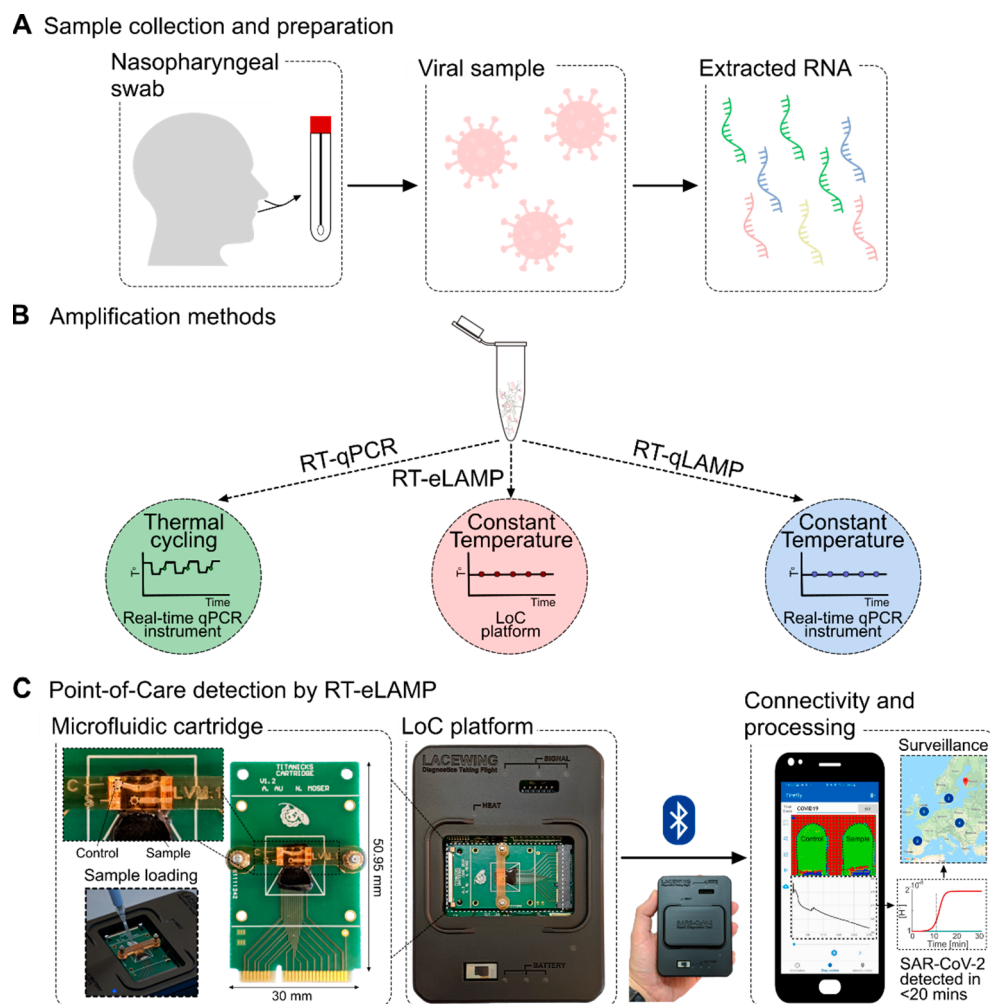


Figure 1. SARS-CoV-2 diagnostic workflow. (A) Sample collection and preparation illustrating nasopharyngeal swab and RNA extraction. (B) Nucleic acid amplification methods for SARS-CoV-2 RNA detection used in this study (RT-qPCR, RT-qLAMP, and RT-eLAMP). Thermal profiles are illustrated for comparison of the assays. (C) Point-of-care diagnostics by RT-eLAMP showing the proposed handheld LoC platform including the microfluidic cartridge with control and sample inlets, and the smartphone-enabled application for geolocalization and real-time visualization of results.

from low sensitivity and specificity. Currently, reverse transcriptase polymerase chain reaction using a real-time benchtop platform (RT-qPCR) is considered the gold standard for COVID-19 diagnosis due to its capability to detect the presence of SARS-CoV-2 RNA close to the onset of symptomatic illness which is critical for isolation. Two RT-qPCR kits have stood out as a reference to most studies, respectively developed by the CDC and the Institut Pasteur (with WHO approval).^{10,12} While these kits are restricted to equipped health centers and are limited by procurement delays, isothermal methods such as reverse transcriptase recombinase polymerase amplification (RT-RPA) or loop-mediated isothermal amplification (RT-LAMP) are an alternative that do not require thermal cycling and provide results within an hour.^{13–23}

These methods are ideal for PoC applications as they (i) reduce turnaround time from sample-to-result, (ii) reduce hardware complexity, (iii) can rapidly respond to emergent strains, and (iv) provide high sensitivity and specificity.^{24–26} However, most of them still rely on fluorescence-based detection which represents a barrier to the implementation of portable devices for SARS-CoV-2 PoC diagnostics.

Alternative sensing technologies based on isothermal amplification which do not require trained personnel or lab-based equipment have been developed but not yet applied to COVID-19.^{27,28} Recently, we have reported an embedded lab-on-chip (LoC) device for label-free electrochemical biosensing applications^{26,29} which consists of ion-sensitive field-effect transistors (ISFETs) manufactured in unmodified complementary metal-oxide-semiconductor (CMOS) technology.³⁰ This device has integrated thermal management and is capable of nucleic acid detection by monitoring pH changes that occur during nucleic acid amplification and are compatible with isothermal assays. The platform demonstrates versatility to a wide range of targets and is compatible with real-time RT-LAMP (RT-eLAMP) and different sample types when coupled with a sample preparation module. Additionally, its use of standard electronic components promotes scalability and portability which ideally match the requirements of portable diagnostics.

In this work, we designed and optimized an RT-LAMP assay targeting the *nucleocapsid* (N) gene of SARS-CoV-2 based on collated sequences from available databases.³¹ To validate the assay, we used a real-time benchtop instrument (RT-qLAMP)

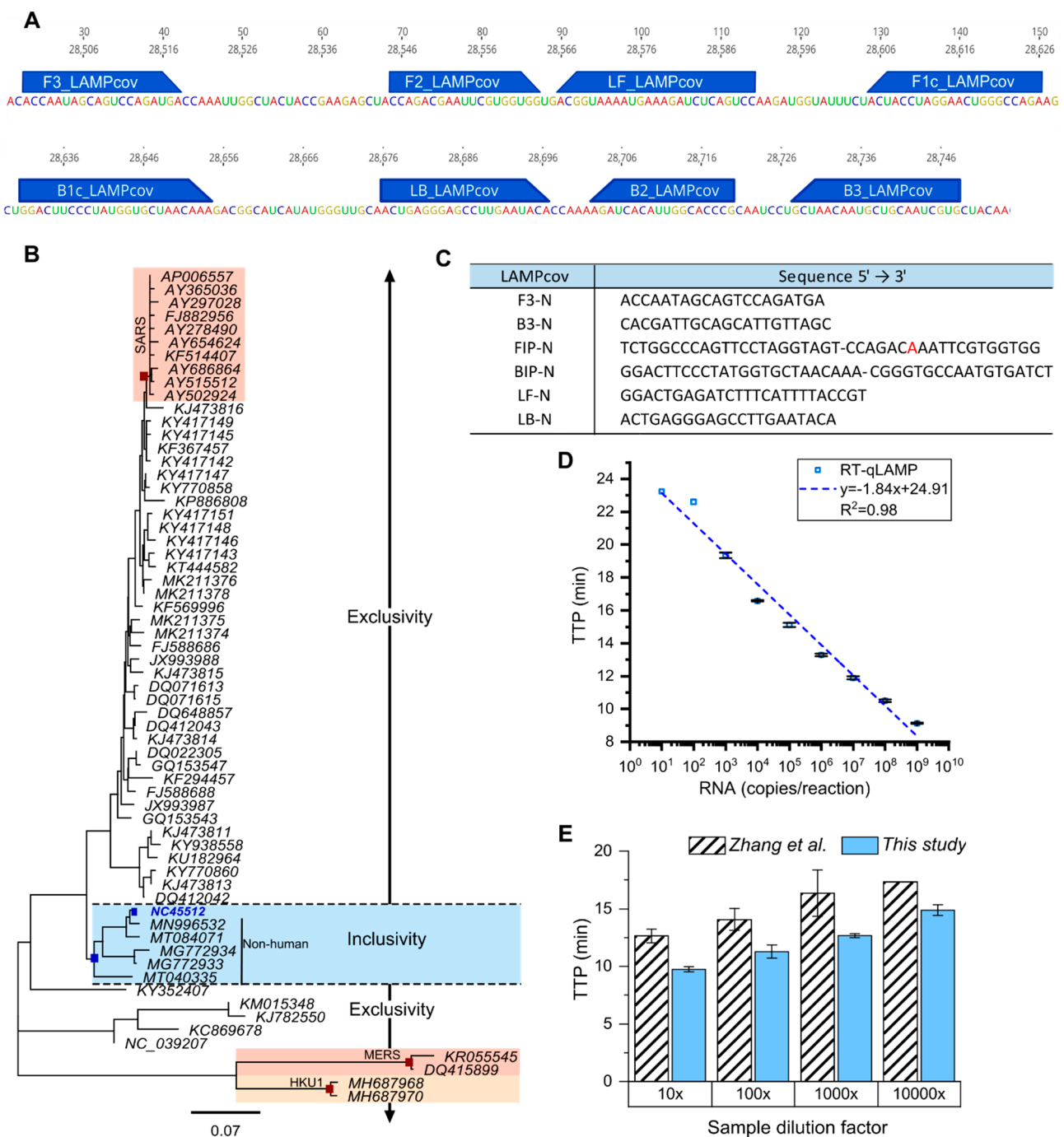


Figure 2. Phylogenetic analysis and LAMPcov assay design. (A) Reference sequence NC_45512 SARS-CoV-2 showing priming regions. (B) Phylogenetic tree showing the specificity of the amplicon for SARS-CoV-2 detection. Clades shaded in blue include the reference sequence NC_45512. Clades highlighted in light red include HKU1, SARS, and MERS, all distant from the inclusivity clade. (C) Sequences of primers of the LAMPcov assay. One mismatch was introduced in F2 to avoid hairpin formation of the primer (in red). (D) Standard curve with RT-qLAMP using a control RNA at concentrations ranging between 10^1 and 10^9 copies per reaction. (E) Comparison between our assay (blue bars) and the published assay by Zhang et al.¹³ (stripped bars). Concentrations (dilution factor) of a clinical sample are plotted against TTP (min).

and screened 183 clinical samples obtained from nasopharyngeal, throat, and nose swabs of symptomatic patients. The results were compared with RT-qPCR,¹² which was used as a gold standard. The RT-qLAMP assay showed a sensitivity of 90.55% and specificity of 100% with a limit of detection of 10 copies per reaction and average positive detection times of 15.45 ± 4.43 min. Furthermore, we implemented the developed RT-LAMP assay on our ISFET-based LoC platform for rapid PoC detection (Figure 1) screening 52 samples,

including positive ($n = 34$) and negative ($n = 18$) isolates. Results obtained by both instruments were comparable (p -value > 0.05), demonstrating the capability of our handheld diagnostic platform paired with a smartphone application to rapidly identify and quantify the presence of SARS-CoV-2 RNA with high reliability. This constitutes the first handheld molecular diagnostic for SARS-CoV-2 detection within 20 min from extracted RNA. Portable diagnostics with secure cloud

Table 1. Results Obtained with RT-qPCR and RT-qLAMP

cat. ^a	RT-qPCR C _t range (cycles)	RNA conc. ^b (copies/ μ L)	samples (n)	RT-qPCR	RT-qLAMP
				C _t \pm STD (cycles)	C _t \pm STD (min)
H	17–22.9	2 \times 10 ⁶ to 3 \times 10 ⁴	13	20.20 \pm 1.82	10.08 \pm 0.83
UM	23–28.9	3 \times 10 ⁴ to 5 \times 10 ²	36	26.51 \pm 1.54	12.55 \pm 1.41
LM	29–34.9	5 \times 10 ² to 8	52	31.78 \pm 1.69	16.47 \pm 3.97
L	>35	<8	26	36.51 \pm 0.88	21.64 \pm 4.17
NEG	NEG		56		
TOTAL			183		

^aResults are classified into categories (cat.) based on RT-qPCR C_t values. H, high; UM, upper-medium; LM, lower-medium; L, low; NEG, negative. ^bRNA estimated concentration (copies/ μ L of eluted sample volume) based on RT-qPCR standard curve $y = -3.30x + 37.98$.

connectivity will enable real-time case identification and epidemiological surveillance.

RESULTS

Optimization of LAMP Assay and Phylogenetic Analysis for RNA Detection of SARS-CoV-2. We have designed and optimized an RT-LAMP assay targeting the N gene of SARS-CoV-2, named LAMPcov. The N gene was selected as the optimal target since it is conserved across available sequences and more resilient to emergent mutations.³² The LAMP assay reported by Zhang et al.¹³ was used as reference for the design of our assay. Other available LAMP assays for COVID-19 have been summarized in Table S1. The LAMPcov assay was designed and optimized manually based on phylogenetic analysis of SARS-CoV-2 sequences and other related viruses (Figure 2B). Primer sequences and the location in the gene can be found in Figure 2A,C. Viral sequences were retrieved from the NCBI database using nucleotide BLAST (BLASTn suite) with the amplicon of the LAMPcov assay as the query. Additionally, complete genomic sequences specific to SARS-CoV-2 were retrieved from GISAID EpiCov. A total of 8921 sequences were collated from both databases, including sequences from different countries such as China, USA, and United Kingdom. Alignments of all retrieved SARS-CoV-2 sequences were performed to evaluate *in silico* the coverage of the developed LAMP assay. Priming regions were mapped in the alignment, and mismatches were found in only 195 sequences out of 8866. These sequences differ from the reference sequence by a maximum of 2 nucleotides which indicates that our target region is specific for SARS-CoV-2 detection (Figures S1 and S2). Furthermore, to evaluate the absence of cross-reactivity with other related viruses, a tree was built based on phylogenetic analysis of unique sequences ($n = 55$) using as a reference the sequence NC_045512 (Figure 2B). A clade including SARS-CoV-2, bat, and pangolin coronaviruses is visible in the lower part of the tree. As previously described,^{4,33} bat coronavirus sequences (bat-SL-CoVZC45, bat-SL-CoVZXC21) are highly similar to the human strain. Most investigations based on genomic sequencing point toward bats and pangolins as the origin of SARS-CoV-2 with evolutionary pathways still to be established.⁴ Therefore, nonhuman strains included in this clade are not anticipated to impact the outcome of the diagnostic results. Other human-infective viruses, including hCoVs such as SARS or MERS, form clades that are located at significantly higher distances. We demonstrate *in silico* the absence of cross-reactivity with other hCoVs and other related viruses based on the high number of mismatches present within the amplicon region of the proposed assay (Figure S3). These sequences

present an identity percentage below 91.4% within the BLAST hits.

Analytical sensitivity of the proposed RT-qLAMP assay is shown in Figure 2D. Time-to-positive (TTP) values ranged between 9 and 24 min, with a limit of detection of 10 copies per reaction. A standard was built ($y = -1.84x + 24.91$) showing a correlation of $R^2 = 0.98$. The LAMP assay developed by Zhang et al.¹³ is included as a reference in Figure 2E. The speed of our assay was increased by an average of 20% with a comparable sensitivity. Overall, results presented in Figure 2 indicate that the proposed LAMPcov assay will not cross-react with other hCoVs or other related viruses and will be able to detect SARS-CoV-2 with high analytical specificity and sensitivity.

Performance Comparison of RT-qPCR and RT-qLAMP with Clinical Samples. A total of 183 clinical samples obtained from nasopharyngeal, throat, or nose swabs were collected from a West London Hospital Laboratory (United Kingdom). Samples were tested with the developed LAMPcov assay and two of the PCR-based assays recommended by the CDC, the N and the RNase P assays.^{10,12} Calculated concentrations based on RT-qPCR and RT-qLAMP standards are detailed in Table S2. RT-qPCR results with the N assay were used as a reference to classify the samples into five categories (high, upper-medium, lower-medium, low, and negative) based on the C_t values obtained (Table 1). C_t was determined by the cycle-threshold method using 0.2 as the fluorescence cutoff value. This classification considered a 6 cycles difference per category, which is equivalent to approximately 100-fold dilution. Results obtained with RT-qLAMP and RT-qPCR are summarized in Table 2. Sensitivity and specificity were 91% and 100% for RT-qLAMP, respectively. From the 183 samples, both RT-qPCR and RT-qLAMP detected 54 samples as negative and 115 as positive. A

Table 2. Sensitivity and Specificity of RT-qLAMP Compared to RT-qPCR for SARS-CoV-2 Detection

assay	RT-qPCR positive (n)	RT-qPCR negative (n)	sensitivity ^a (%)	specificity ^b (%)
RT-qLAMP positive (n)	115	0 ^c	90.55	100
RT-qLAMP negative (n)	12	54	90.55	100

^aSensitivity calculated based on $SEN (\%) = \frac{TP}{TP + FN} \times 100$ ^bSpecificity calculated based on $SPE (\%) = \frac{TN}{TN + FP} \times 100$ ^cMelting curve analysis (Figure S4) confirmed specificity of the product for 2 samples detected only by RT-qLAMP, omitted in the table for sensitivity and specificity analysis.

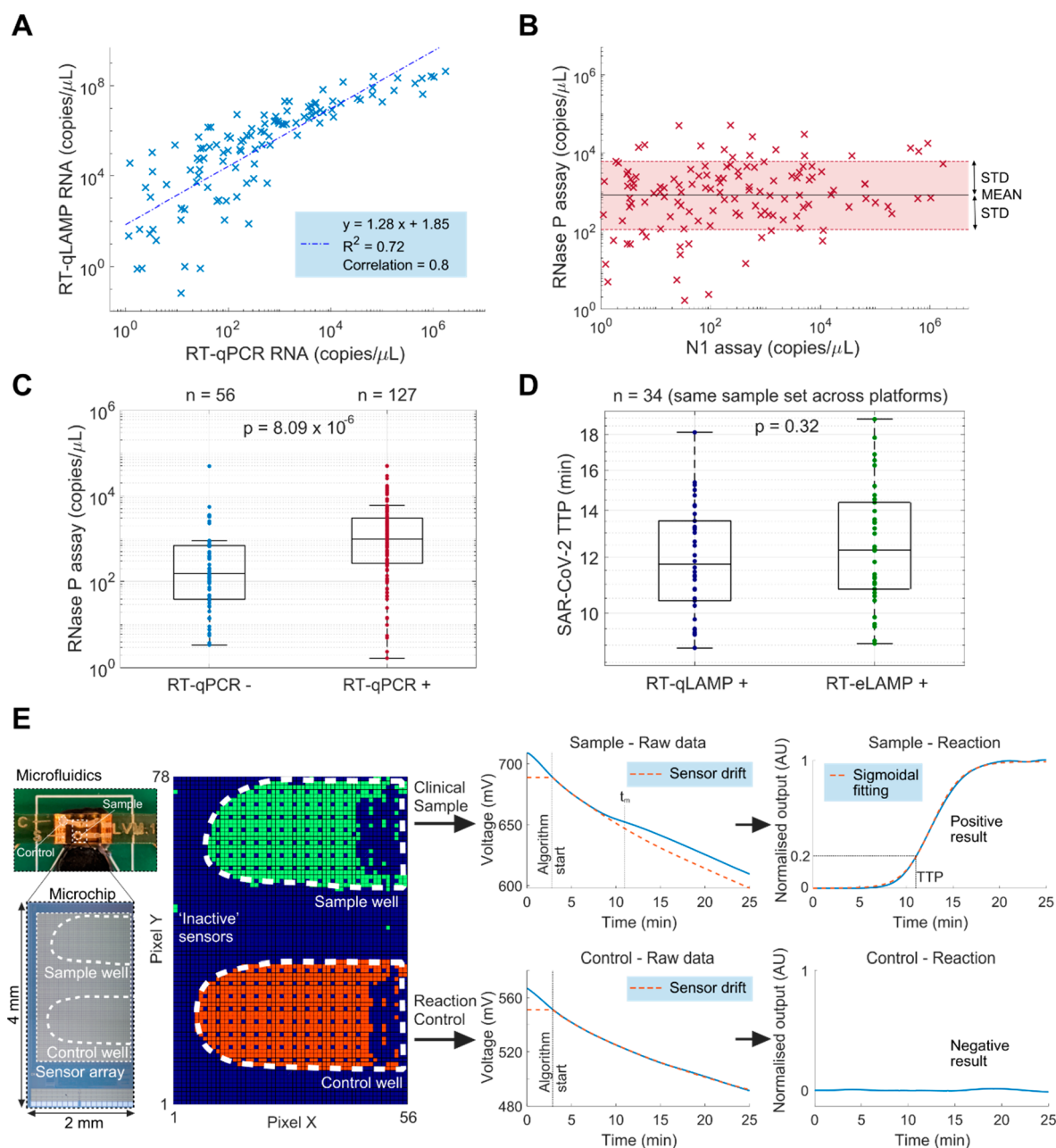


Figure 3. Clinical validation using RT-qPCR, RT-qLAMP, and RT-eLAMP. (A) Correlation between RT-qPCR and RT-qLAMP based on the estimated sample concentration (copies/ μL of eluted sample volume), $n = 115$. (B) Correlation between RNase P and viral RNA concentration of the positive clinical samples (copies/ μL of eluted sample volume) to indicate quality of extraction across all of the cohort, $n = 127$. (C) Boxplot distribution of RNase P concentration (copies/ μL of eluted sample volume) across negative ($n = 56$) and positive ($n = 127$) clinical samples by RT-qPCR. The calculated p -value between both groups was below 0.05 (p -value = 8.09×10^{-6}). (D) Boxplot distribution of TTP for the RT-qLAMP and RT-eLAMP demonstrating the performance of the LoC platform ($n = 34$ positive samples). The calculated p -value between both groups is higher than 0.05 (p -value = 0.32). It is important to note that 18 negative samples were confirmed by RT-qLAMP and RT-eLAMP. (E) Example overview of data processing steps for sample 179 to extract amplification curves from sample and control wells on the LoC platform during RT-eLAMP. The spatial image illustrates the microchip ISFET sensing array output (4368 sensors, 2×4 mm) on the single-use cartridge where the averaged sensor signals in each well demonstrate, respectively, amplification with a TTP of 10.63 min (sample) and no amplification (control).

total of 12 samples were detected as positive only by RT-qPCR (negative by RT-qLAMP), and 2 were detected as positive only by RT-qLAMP (negative by RT-qPCR). The 14 misclassified samples belong to the “Low” concentration group which could justify the discrepancy between the 2 assays. Furthermore, the 2 samples detected only by RT-qLAMP were confirmed as true positive by melting curve analysis (Figure S4); therefore, they were not considered false

positive and were omitted from the sensitivity and specificity calculations (Table 2).

To further evaluate the performance of the proposed RT-qLAMP assay in comparison to RT-qPCR, the correlation between the two methods was computed by applying linear regression. A total of 115 samples were detected by both methods and included for this analysis. Viral load was calculated based on RT-qPCR and RT-qLAMP standards

previously built with a control RNA (obtained from SARS-CoV-2 viral culture). Results are summarized in Figure 3A where calculated viral loads with each of the methods were plotted. The x -axis corresponds to viral load by RT-qPCR, and the y -axis corresponds to viral load by RT-qLAMP. The obtained correlation is 0.8 with an $R^2 = 0.72$ ($n = 115$). Furthermore, the RNase P assay recommended by the CDC¹² was used to evaluate the quality of the extracted RNA and verify the human origin of the clinical samples. RNase P concentration was calculated based on an RT-qPCR standard previously built with a positive control provided by IDT (Hs_RPP30). The homogeneous distribution of the RNase P concentration across RT-qPCR positive ($n = 127$) samples for SARS-CoV-2 indicates that all samples present a similar quality after RNA extraction (Figure 3B). However, distribution of RNase P concentration is significantly different (p -value = 8.09×10^{-6}) between RT-qPCR positive ($n = 127$) and negative ($n = 56$) samples for SARS-CoV-2 (Figure 3C). This indicates that the quality of RNA might be different between both groups which could lead to an increased number of false negatives. Overall, despite the lower sensitivity of the RT-qLAMP assay compared to RT-qPCR, the proposed isothermal assay detected two samples that were missed by RT-qPCR. These samples were specific (by melting curve analysis) and could not be considered as false positives. Therefore, a 100% specificity was preserved.

The RT-qPCR assay also required an additional 40 min compared to RT-qLAMP for sample screening, as at least 60 min are needed to complete the 45 recommended cycles. In particular, the average TTP values within the “High” concentration group are 20.20 ± 1.82 cycles and 10.08 ± 0.83 min, with RT-qPCR and RT-qLAMP, respectively, and the average TTP values of the samples within the “Low” concentration group are 36.51 ± 0.88 cycles and 21.64 ± 4.17 min, respectively. Furthermore, RT-qPCR relies on thermal cycling, which limits its implementation for SARS-CoV-2 diagnostics at the PoC.

Rapid Point-of-Care Detection of SARS-CoV-2 Using a Lab-on-Chip Device. A subset of 52 samples (34 positive and 18 negative) were tested by RT-eLAMP to characterize the performance of our PoC test compared to a benchtop instrument. The sample size was calculated based on the equation reported by Banoo et al.³⁴ TTP values observed for each sample are included in Table S3. The results shown in Figure 3D demonstrate good correlation between the TTP obtained by RT-qLAMP and RT-eLAMP, achieving, respectively, average TTP values of 12.10 ± 2.20 min and 12.68 ± 2.56 min. The calculated p -value is above 0.05 (p -value = 0.32) demonstrating that there is no statistical difference in the performance of both platforms. This validates the incorporation of our new RT-qLAMP assay with our LoC platform.

The single-use cartridge consists of a CMOS ISFET microchip (array of 78×56 sensors, 2×4 mm) with a bespoke microfluidic module to accommodate two wells on the sensing surface, for sample and control reactions. An initial calibration phase relying on machine learning and spatial clustering techniques was run on the 4368 time series from the sensor outputs to filter out sensors which were not in contact with the solution or out of readout range, labeled “inactive” sensors (shown in dark blue in Figure 3E). The remaining sensors match the positions of the sample and control wells. The algorithm averaged the output of the sensors within each well and performed drift compensation. To accurately identify

the voltage change as a result of pH variations, we relied on (i) identifying the time of maximum derivative, and (ii) performing compensation of sensor drift based on exponential interpolation to extract information on nucleic acid amplification.^{26,30,35} The algorithm produced a standard amplification curve for each well, monitoring the proton concentration in real time during the reaction and hence the increase in DNA copies. Sigmoidal fitting was performed on the compensated sensor signal for detected amplifications to reflect the dynamics of nucleic acid amplification. In each experiment, we ensured that no amplification occurred in the control well within 20 min and quantified the presence of SARS-CoV-2 RNA in the clinical sample well by extracting the TTP based on 0.2 thresholding after normalization. Estimated concentrations with RT-eLAMP are provided in Table S3.

The integrated sensors and novel algorithms allow the detection and quantification of the presence of SARS-CoV-2 in the extracted clinical samples, with a similar performance between the RT-qLAMP and the RT-eLAMP. Adding to the benefits of speed and portability, the LoC platform was connected to a custom smartphone application compatible with any Android device and designed to acquire and process the sensor data during the reaction (Figure 1C). Upon termination of the reaction, the data was synchronized to a secure Amazon cloud server (AWS), and the GPS location from the phone was used to locate the experiment on a map.

DISCUSSION

Stringent mitigation measures have been implemented in an effort to limit the spread of SARS-CoV-2. With 79.5 million reported cases,³⁶ the COVID-19 pandemic has been deemed a global health emergency, characterized by the uncontrolled rate of person to person transmission and ongoing increase of cases.^{37,38} Rapid PoC diagnostics are more critical than ever, helping to identify and track the spread of the disease. In this paper, we combined LAMP with an *in-house* LoC device to develop a rapid PoC diagnostic test (<20 min) for the detection of SARS-CoV-2 RNA from extracted samples. The proposed RT-LAMP assay, named LAMP_{cov}, was designed based on phylogenetic analysis of 8921 sequences retrieved from NCBI and GISAID databases.^{31,39} The N gene was selected as the target due to its high specificity for SARS-CoV-2 detection, resilience to mutations and high conservation among reported SARS-CoV-2 sequences from different countries including United Kingdom, China, and USA (Figure 2). A total of 183 clinical samples were screened by RT-qLAMP and RT-qPCR using the kit recommended from the CDC (N and RNase P assays).¹² Currently, RT-qPCR is considered the gold standard for SARS-CoV-2 detection. However, this method is hindered by the need for laboratory-based equipment, trained personnel, thermal-cycling instruments, and procurement delays in public health institutions such as hospitals or diagnostic centers where availability of these tests is restricted to. Although the RT-qLAMP assay showed a 91% sensitivity compared to RT-qPCR, specificity was 100%. The two samples that were only detected by RT-qLAMP were not considered false positives as specificity of the reaction was confirmed by melting curve analysis. It is important to notice that RNase P analysis showed a significant difference between positive and negative samples (p -value < 0.05) which could lead to an increase in the number of false negatives. RT-qLAMP also showed a faster turnaround time with an average TTP of 15.45 ± 4.43 min. Therefore, the

proposed assay is an ideal alternative to RT-qPCR for SARS-CoV-2 PoC diagnostic applications. The LAMPcov assay was also successfully implemented on the *in-house* developed LoC device, and a subset of samples ($n = 52$) were screened. Results obtained on the LoC platform presented a good correlation compared to the experiments carried out in a commercial PCR thermal-cycling instrument (p -value > 0.05), confirming the robustness of the assay and the device. Currently, very few portable instruments are available for PoC diagnostics. Most of the reported rapid diagnostic tests rely on antigen or antibody detection. Antigen detection tests commonly suffer from low sensitivity, with high false negative rates reported. Nevertheless, they are potential candidates as first line rapid tests if sensitivity is improved. Antibody tests, more commonly known as serological tests, rely on the detection of antibodies such as IgA, IgM, and IgG which are the product of the immune system response to SARS-CoV-2. However, several days/weeks are needed for the antibodies to be released by the immune system, shifting the detection window away from the onset of symptomatic illness. Unfortunately, it is during this window that isolation is most critical. Furthermore, antibodies are often not SARS-CoV-2 specific, leading to a high false positive rate.^{9,40}

The latest PoC diagnostic tests based on nucleic acid amplification methods that have been authorized by the FDA (emergency use authorization) include (1) Abbott ID NOW COVID-19 (Abbott), (2) Xpert Xpress SARS-CoV-2 (Cepheid), and (3) AcculaSARS-Cov-2 Test (Mesa Biotech Inc.).⁴¹ The first two are quantitative tests, and the last one is qualitative. All of them have an integrated RNA extraction step and provide a diagnosis within 15–45 min. Although these instruments are sample-to-results devices, they are not portable and may not be affordable for most clinics in resource-limited settings. Due to leveraging on the semiconductor industry, the rapid PoC diagnostic test proposed in this work offers a portable and affordable solution. In contrast to a recently reported lateral flow test based on CRISPR–Cas12,³⁷ the presented device is also a quantitative test, providing information on the viral load, which can be an important indicator of the patient's infectivity. Furthermore, the proposed PoC diagnostic test can be rapidly adapted for the detection of other respiratory pathogens or infectious diseases^{25,26,30} as only a target-specific LAMP assay has to be incorporated. This inherent capability promotes versatility and improves scalability, offering a wide range of applications that can be easily integrated for the simultaneous multiple detection of pathogens. This versatility further improves when considering that it can be integrated as a two-step approach with sample preparation methods or modules to obtain a sample-to-result diagnostic test which can be used for a variety of targets, from any sample type and without the need for trained personnel.⁴² This highlights the opportunity to consider this device for use in the community, where it has the potential to offer ease of use and rapid detection through a custom smartphone app. Given the additional benefit of the incorporated geolocalization feature, we envision this PoC device as a valuable tool for epidemiological surveillance and infection tracking for not only SARS-CoV-2 but also other infectious diseases.

MATERIALS AND METHODS

Study Design. The goal of this study was to demonstrate a PoC diagnostic test based on LAMP and semiconductor technology to detect the presence of SARS-CoV-2 from

extracted RNA. To evaluate the performance of the proposed diagnostic test compared to reference methods, a total of 183 extracted RNA samples from nasopharyngeal, throat, and nose swabs were screened by RT-qLAMP and RT-qPCR (CDC assay).¹² All studies were conducted in accordance with the ethical approval (20/HRA/1561; DOCUMAS 20SM5875).

To estimate the number of samples required to be screened on the LoC platform, the following formula was used:³⁴

$$n \geq \frac{1.96^2 p(1-p)}{x^2} \quad (1)$$

where p is the suspected sensitivity, and x is the desired margin of error. We define the true-positive rate (sensitivity) as the proportion of SARS-CoV-2 positive which is correctly identified by the LoC platform compared to the benchtop instrument. We suspected the sensitivity and specificity of the RT-eLAMP assay to be 90% with a desired margin of error of 15%. Under these conditions, the number of required samples is 15.36 (rounded up to 16) per group. In total for the LoC experiments, we have tested 52 samples (34 positive and 18 negative).

Phylogenetics Analysis. Genomic viral sequences were retrieved from NCBI using nucleotide BLAST with the amplicon of the proposed RT-LAMP assay as the query ($n = 4506$). A total of 4451 sequences were specific for SARS-CoV-2, and 55 sequences were related to other viruses. Complete genomic sequences specific to SARS-CoV-2 were collated from the GISAID EpiCov database using as a query human host and different locations including United Kingdom, China, and USA ($n = 4415$). Nucleotide sequence alignment was performed using the MUSCLE algorithm⁴³ in Geneious Prime software⁴⁴ v2019.04 using as a reference the sequence NC_045512. The neighbor-joining method was used to build a phylogenetic tree with 100 bootstraps replicates using the alignment of unique sequences retrieved from the Blastn query in NCBI ($n = 55$) with NC_045512 as a reference for SARS-CoV-2. Accession numbers are listed in Figures S1–S3.

LAMP Assay Development. Primers were designed and optimized manually based on the Zhang et al.¹³ assay and phylogenetics analysis of SARS-CoV-2 sequences and other related viruses. Developed primers were analyzed *in silico* for the presence of hairpins, dimers, and cross-dimers using NUPACK,⁴⁵ IDT OligoAnalyzer software, and the ThermoFisher Multiple Primer analyzer tool. Melting temperatures (T_m) were calculated using the J. SantaLucia thermodynamics table.⁴⁶ All primers were synthesized by IDT, and sequences are listed in Figure 2.

Clinical Samples and Controls. Clinical nasopharyngeal, throat, and nose swabs were collected and processed by the Microbiology laboratory at a West London Hospital Laboratory (United Kingdom). A total of 183 samples were collected, and RNA was extracted using AusDiagnostics MT extractor with an elution volume ranging from 50 to 200 μ L (AusDiagnostics) following manufacturer instructions.

Quantified RNA from the viral culture was used as a control. VeroE6 cells were infected with A/SARS-CoV-2/England/IC19/2020 at an MOI of 0.01 and incubated in 5% CO₂ at 37 °C. After 1 h of virus adsorption, the virus inoculum was removed, and the cells were washed in phosphate-buffered saline (PBS) and replenished with Dulbecco's modified Eagle's medium (DMEM) (Gibco, Thermo Fisher Scientific) supplemented with 1% penicillin–streptomycin (Thermo

Fisher Scientific) and 1% MEM nonessential amino acids (Gibco, Thermo Fisher Scientific) in 5% CO₂ at 37 °C. 48 h later, the supernatant was removed, and total RNA was extracted using TRIzol reagent (Invitrogen) followed by column purification using the RNeasy RNA Mini kit (Qiagen).

Reaction Conditions. RT-qPCR Reaction. Experiments were carried out in duplicates with a final volume of 10 μ L per reaction using two of the assays recommended by the CDC, the N assay (N1 primer mix) and the RNase P assay, with the GoTaq 1-Step RT-qPCR kit (Promega). Each mix contained the following: 10 μ L of 2 \times GoTaq qPCR master mix, 0.4 μ L of 50 \times GoScript RT mix for 1-Step RT-qPCR, 1.2 μ L of 16.6 \times N1/RNase P assay primer mix by the CDC [Forward Primer (20 μ M), Reverse Primer (20 μ M), Probe (5 μ M)], 4 μ L of extracted RNA, and enough nuclease-free water (GoTaq 1-Step RT-qPCR kit, Promega) to bring the volume to 20 μ L. Reactions were performed following the recommendations of the manufacturer: 15 min at 63 °C for cDNA conversion, 2 min at 95 °C for AMV deactivation, and 45 cycles at 95 °C for 15 s and 55 °C for 45 s. Reactions were plated in 96-well plates and loaded into a LightCycler 96 real-time PCR system (LC96) (Roche Diagnostics). The N1 assay and the RNase P assay were purchased from IDT and used following the recommendations of the manufacturer.

RT-qLAMP Reaction. Experiments were carried out in duplicates with a final volume of 10 μ L per reaction. Each mix contained the following: 2 μ L of 10 \times isothermal buffer (New England Biolabs), 1.20 μ L of MgSO₄ (100 mM stock), 2.80 μ L of dNTPs (10 mM stock), 0.50 μ L of BSA (20 mg/mL stock), 3.20 μ L of Betaine (5 M stock), 0.50 μ L of SYTO 9 Green (20 μ M stock), 1.25 μ L of Bst 2.0 DNA polymerase (8000 U/mL stock), 0.64 μ L of AMV (25 U/ μ L stock, Promega), 0.20 μ L of Rnase inhibitor (20 U/ μ L stock, ThermoFisher Scientific), 4 μ L of extracted RNA, 1 μ L of 10 \times LAMP primer mixture (20 μ M of BIP/FIP, 10 μ M of LF/LB, and 2.5 μ M B3/F3), and enough nuclease-free water (ThermoFisher Scientific) to bring the volume to 20 μ L. Reactions were performed at 63 °C for 30 min. One melting cycle was performed at 0.1 °C/s from 65 °C up to 97 °C for validation of the specificity of the products. Reactions were plated in 96-well plates and loaded into a LightCycler 96 real-time PCR system (LC96) (Roche Diagnostics).

RT-eLAMP Reaction. Experiments were carried out at a final volume of 5 μ L per reaction. Each mix contained the following: 0.50 μ L of 10 \times isothermal pH-based buffer (pH 8.5–9), 0.30 μ L of MgSO₄ (100 mM stock), 0.28 μ L of dNTPs (25 mM stock), 0.30 μ L of BSA (20 mg/mL stock), 0.13 μ L of NaOH (200 mM stock), 0.80 μ L of Betaine (5 M stock), 0.02 μ L of Bst 2.0 DNA polymerase (120 000 U/mL stock), 0.13 μ L of AMV (25 U/ μ L stock, Promega), 0.05 μ L of Rnase inhibitor (20 U/ μ L stock, ThermoFisher Scientific), 2 μ L of extracted RNA, and 0.50 μ L of 10 \times LAMP primer mixture (20 μ M of BIP/FIP, 10 μ M of LF/LB, and 2.5 μ M B3/F3). Experiments were performed at 63 °C for 30 min. Reactions were loaded into a disposable cartridge, and experiments were carried out using our *in-house* LoC platform.

Lab-on-Chip Platform. We translated the RT-LAMP assay on a portable lab-on-chip platform illustrated in Figure 1C and achieving RT-eLAMP at the PoC. The platform relies on a single-use cartridge which combines state-of-the-art microchip technology and microfluidic developments. The RT-LAMP assay was performed on a large array of over 4368 sensors called ion-sensitive field-effect transistors (ISFETs) monitoring

nucleic acid amplification through the release of protons in reaction associated with nucleotide incorporation during LAMP. Bolted onto each cartridge was a 3D printed microfluidic manifold, printed using a standalone 3D printer from 3D Systems, in their transparent biocompatible capable (ISO 10993-5 and 10993-10) MED-AMB-10 resin. Each manifold contained two internal microfluidic channels, which distributed 5 μ L of sample and 5 μ L of control reaction mix onto two separate designated sensing areas of the chip surface. Sealing between the manifold and chip surface was accomplished through laser-cut double-stick Tessa adhesive gaskets, with a Ag/AgCl reference electrode (chloridized 0.03 mm Ag wire) running through each reaction well between the chip surface and tape gasket. The adhesive gasket and printed resin materials were chosen for their low reaction inhibition, determined experimentally.

The battery-powered portable LoC device performed isothermal temperature regulation of the solution with a Peltier module in contact with the cartridge. An embedded microcontroller was used to implement the PID controller and transmit the data via Bluetooth to a custom smartphone application developed on AndroidOS. The app shared data on a secure cloud server hosted by Amazon Web Services and performed geotagging using the phone GPS.

Lab-on-chip reactions were performed by injecting sample and control reaction mix onto each of the two designated wells (sample and control wells). Sample reaction mix contained the reaction mix described for RT-eLAMP including extracted RNA. Control reaction mix did not include extracted RNA but nuclease-free water instead. Reactions were performed for 30 min, and data was recorded *in situ* in real-time. The sensor data was processed in MATLAB as follows:^{30,47} (i) We compensated for sensor drift based on an exponential interpolation. (ii) We converted the voltage output to a pH variation using the measured sensitivity of standard CMOS technology. (iii) We linearized the output to reflect the change in protons and hence DNA copies during the reaction. (iv) We normalized the curve, and (v) we extracted the TTP based on cross-thresholding at 0.2.

Data Analysis and Statistics. Data analysis was performed using MATLAB (R2018b) and OriginPro 2019. All the TTP values are reported as mean \pm std using built in functions in MATLAB. A one-sample Kolmogorov–Smirnov test was performed to verify that the data is normally distributed; a two-sample F-test was performed to verify that the data is normally distributed with equal variance. A two-sample Student's *t* test was performed for comparison between groups which present a normal distribution with equal mean and variance. A *p*-value \leq 0.05 was considered as a threshold for statistical significance.

■ ASSOCIATED CONTENT

Supporting Information

The Supporting Information is available free of charge at <https://pubs.acs.org/doi/10.1021/acscentsci.0c01288>.

Detailed alignments and clinical data (PDF)

■ AUTHOR INFORMATION

Corresponding Author

Jesus Rodriguez-Manzano – Department of Infectious Disease, Faculty of Medicine and Department of Electrical and Electronic Engineering, Faculty of Engineering, Imperial

College London, London SW7 2AZ, United Kingdom;
 orcid.org/0000-0002-2583-8366; Email: j.rodriquez-
 manzano@imperial.ac.uk

Authors

Kenny Malpartida-Cardenas – Department of Electrical and Electronic Engineering, Faculty of Engineering, Imperial College London, London SW7 2AZ, United Kingdom;

orcid.org/0000-0002-3874-8810

Nicolas Moser – Department of Electrical and Electronic Engineering, Faculty of Engineering, Imperial College London, London SW7 2AZ, United Kingdom

Ivana Pennisi – Department of Infectious Disease, Faculty of Medicine and Department of Electrical and Electronic Engineering, Faculty of Engineering, Imperial College London, London SW7 2AZ, United Kingdom

Matthew Cavuto – Department of Electrical and Electronic Engineering, Faculty of Engineering, Imperial College London, London SW7 2AZ, United Kingdom

Luca Miglietta – Department of Electrical and Electronic Engineering, Faculty of Engineering, Imperial College London, London SW7 2AZ, United Kingdom

Ahmad Moniri – Department of Electrical and Electronic Engineering, Faculty of Engineering, Imperial College London, London SW7 2AZ, United Kingdom

Rebecca Penn – Department of Infectious Disease, Faculty of Medicine, Imperial College London, London SW7 2AZ, United Kingdom

Giovanni Satta – Imperial College Healthcare NHS Trust, Hammersmith Hospital, London W12 0HS, United Kingdom

Paul Randell – Imperial College Healthcare NHS Trust, Hammersmith Hospital, London W12 0HS, United Kingdom

Frances Davies – Department of Infectious Disease, Faculty of Medicine, Imperial College London, London SW7 2AZ, United Kingdom

Frances Bolt – Department of Infectious Disease, Faculty of Medicine, Imperial College London, London SW7 2AZ, United Kingdom

Wendy Barclay – Department of Infectious Disease, Faculty of Medicine, Imperial College London, London SW7 2AZ, United Kingdom

Alison Holmes – Department of Infectious Disease, Faculty of Medicine, Imperial College London, London SW7 2AZ, United Kingdom; Imperial College Healthcare NHS Trust, Hammersmith Hospital, London W12 0HS, United Kingdom

Pantelis Georgiou – Department of Electrical and Electronic Engineering, Faculty of Engineering, Imperial College London, London SW7 2AZ, United Kingdom

Complete contact information is available at:

<https://pubs.acs.org/10.1021/acscentsci.0c01288>

Author Contributions

P.G., J.R.-M., and A.H. conceptualized and designed the study. K.M.-C., N.M., I.P., M.C., L.M., and A.M. performed the experiments. K.M.-C. and N.M. analyzed the data. G.S., P.R., F.D., F.B. R.P., and W.B. collected the samples and controls used in this study. J.R.-M., K.M.-C., and N.M. wrote the manuscript. All authors reviewed the manuscript. The manuscript was written through contributions of all authors. All authors have given approval to the final version of the manuscript.

Funding

This work was supported by the Imperial College COVID19 Research Fund (G38041 and PSH819 Awards) and the NIHR Imperial Biomedical Research Centre (P80763). We would also like to thank the Imperial College Healthcare NHS Trust microbiology lab for providing the samples. A.H. is a National Institute for Health Research (NIHR) Senior Investigator. The views expressed in this publication are those of the author(s) and not necessarily those of the Department of Health and Social Care NHS, or the National Institute for Health Research. We would also like to acknowledge EPSRC HiPEDS CDT (EP/L016796/1 to K.M.-C.) and EPSRC DTP (EP/N509486/1 to A.M.) for supporting this work. Authors are affiliated with the Department of Health and Social Care, Centre for Antimicrobial Optimisation (CAMO) at Imperial College, London. The authors also acknowledge the support of the National Institute for Health Research Health Protection Research Unit (NIHR HPRU) in Healthcare Associated Infections and Antimicrobial Resistance at Imperial College London in partnership with Public Health England (PHE).

Notes

The authors declare no competing financial interest.

REFERENCES

- (1) World Health Organization (WHO). *WHO coronavirus-2019*. <https://www.who.int/emergencies/diseases/novel-coronavirus-2019> (accessed Dec. 28, 2020).
- (2) Zhong, J.; Tang, J.; Ye, C.; Dong, L. The Immunology of COVID-19: Is Immune Modulation an Option for Treatment? *Lancet Rheumatol.* **2020**, *2* (7), e428–e436.
- (3) Sohrabi, C.; Alsafi, Z.; O'Neill, N.; Khan, M.; Kerwan, A.; Al-Jabir, A.; Iosifidis, C.; Agha, R. World Health Organization Declares Global Emergency: A Review of the 2019 Novel Coronavirus (COVID-19). *Int. J. Surg.* **2020**, *76* (Feb), 71–76.
- (4) Ye, Z. W.; Yuan, S.; Yuen, K. S.; Fung, S. Y.; Chan, C. P.; Jin, D. Y. Zoonotic Origins of Human Coronaviruses. *Int. J. Biol. Sci.* **2020**, *16* (10), 1686–1697.
- (5) Harapan, H.; Itoh, N.; Yufika, A.; Winardi, W.; Keam, S.; Te, H.; Megawati, D.; Hayati, Z.; Wagner, A. L.; Mudatsir, M. Coronavirus Disease 2019 (COVID-19): A Literature Review. *J. Infect. Public Health* **2020**, *13* (5), 667–673.
- (6) Chen, S.-J.; Wang, S.-C.; Chen, Y.-C. Novel Antiviral Strategies in the Treatment of COVID-19: A Review. *Microorganisms* **2020**, *8* (9), 1259.
- (7) Le, T. T.; Cramer, J. P.; Chen, R.; Mayhew, S. Evolution of the COVID-19 Vaccine Development Landscape. *Nat. Rev. Drug Discovery* **2020**, *19* (10), 667–668.
- (8) Mahase, E. Covid-19: UK Approves Pfizer and BioNTech Vaccine with Rollout Due to Start next Week. *BMJ.* **2020**, No. m4714.
- (9) Cheng, M. P.; Papenburg, J.; Desjardins, M.; Kanjilal, S.; Quach, C.; Libman, M.; Dittrich, S.; Yansouni, C. P. Diagnostic Testing for Severe Acute Respiratory Syndrome-Related Coronavirus-2. *Ann. Intern. Med.* **2020**, *172* (11), 726.
- (10) Udugama, B.; Kadhiresan, P.; Kozlowski, H. N.; Malekjahani, A.; Osborne, M.; Li, V. Y. C.; Chen, H.; Mubareka, S.; Gubbay, J. B.; Chan, W. C. W. Diagnosing COVID-19: The Disease and Tools for Detection. *ACS Nano* **2020**, *14* (4), 3822–3835.
- (11) Zhang, K. Clinically Applicable AI System for Accurate Diagnosis, Quantitative Measurements and Prognosis of COVID-19 Pneumonia Using Computed Tomography. *Cell* **2020**, *181* (6), 1423.
- (12) CDC. *Real-Time RT-PCR for Diagnosing COVID 19*. CDC, 2020.
- (13) Zhang, Y.; Odiwuor, N.; Xiong, J.; Sun, L.; Nyaruaba, R. O.; Wei, H.; Tanner, N. A. Rapid Molecular Detection of SARS-CoV-2 (COVID-19) Virus RNA. *medRxiv*, 2020.

- (14) Lamb, L. E.; Bartolone, S. N.; Ward, E.; Chancellor, M. B. Rapid Detection of Novel Coronavirus (COVID-19) by Reverse Transcription- Loop-Mediated Isothermal Amplification. *medRxiv*, 2020. DOI: 10.1101/2020.02.19.20025155
- (15) Mohamed El-Tholoth, H. H.; Bau, J. S. A Single and Two-Stage, Closed-Tube, Molecular Test for the 2019 Novel Coronavirus (COVID-19) at Home, Clinic, and Points of Entry. *ChemRxiv*, 2019. DOI: 10.26434/chemrxiv.11860137.v1
- (16) Lin, Y.; Shanshan, W.; Xiaowen, H.; Xuelong, L.; Xiyang, L.; Shenglong, Y.; Heng, H.; Xue, D.; Xin, L.; Jiyao, L.; Na, L.; Jianmin, L.; Wanzhong, Z.; Vicent, P.; Wei-Hua Chen, X. Y. Rapid Colorimetric Detection of COVID-19 Coronavirus Using a Reverse Transcriptional Loop-Mediated Isothermal Amplification (RT-LAMP) Diagnostic Platform: ILACO. *medRxiv*, 2020. DOI: 10.1101/2020.02.20.20025874
- (17) Xiong, Z.; Xiaoxia, W.; Limei, H.; Ting, C.; Licheng, W.; Huan, L.; Sha, L.; Lvfen, H.; Xiaoying, F.; Shaojin, C.; Mei Xing, H. C.; Wang, Y. Reverse Transcription Loop-Mediated Isothermal Amplification Combined with Nanoparticles-Based Biosensor for Diagnosis of COVID-19. *medRxiv*, 2020.
- (18) Weihua, Y.; Xiaofei, D.; Qingxi, W.; Mingjie, X.; Qianqian, Z.; Yunying, Z.; Huailong, Z.; Li, W.; Yihui, X.; Jun, W.; Shuyi, H.; Min, W.; Fenyang Pei, Y. W. Rapid Detection of SARS-CoV-2 Using Reverse Transcription RT-LAMP Method. *medRxiv*, 2020. DOI: 10.1101/2020.03.02.20030130
- (19) Park, G.; Ku, K.; Baek, S.; Kim, S. J.; Kim, S. I.; Kim, B. Development of Reverse Transcription Loop-Mediated Isothermal Amplification (RT-LAMP) Assays Targeting SARS-CoV-2. *bioRxiv*, 2020. DOI: 10.1101/2020.03.09.983064
- (20) Jiang, M.; Pan, W.; Aratehfar, A.; Fang, W.; Ling, L.; Fang, H.; Daneshnia, F.; Yu, J.; Liao, W.; Pei, H.; Xiaojing, L.; Lass-Flörl, C. Development and Validation of a Rapid, Single-Step Reverse Transcriptase Loop-Mediated Isothermal Amplification (RT-LAMP) System Potentially to Be Used for Reliable and High-Throughput Screening of COVID-19. *medRxiv*, 2020. DOI: 10.1101/2020.03.15.20036376
- (21) Zhu, X.; Ge, Y.; Wu, T.; Zhao, K.; Chen, Y.; Wu, B.; Zhu, F.; Zhu, B.; Cui, L. Co-Infection with Respiratory Pathogens among COVID-2019 Cases. *Virus Res.* **2020**, *285* (April), 198005.
- (22) Ding, X.; Yin, K.; Li, Z.; Liu, C. All-in-One Dual CRISPR-Cas12a (AIOD-CRISPR) Assay: A Case for Rapid, Ultrasensitive and Visual Detection of Novel Coronavirus SARS-CoV-2 and HIV Virus. *bioRxiv*, 2020. DOI: 10.1101/2020.03.19.998724
- (23) Lu, R.; Wu, X.; Wan, Z.; Li, Y.; Zuo, L.; Qin, J.; Jin, X.; Zhang, C. Development of a Novel Reverse Transcription Loop-Mediated Isothermal Amplification Method for Rapid Detection of SARS-CoV-2. *Viol. Sin.* **2020**, *35*, 344.
- (24) Notomi, T.; Okayama, H.; Masubuchi, H.; Yonekawa, T.; Watanabe, K.; Amino, N.; Hase, T. Loop-Mediated Isothermal Amplification of DNA. *Nucleic Acids Res.* **2000**, *28* (12), 63e.
- (25) Malpartida-Cardenas, K.; Miscourides, N.; Rodriguez-Manzano, J.; Yu, L.-S.; Moser, N.; Baum, J.; Georgiou, P. Quantitative and Rapid Plasmodium Falciparum Malaria Diagnosis and Artemisinin-Resistance Detection Using a CMOS Lab-on-Chip Platform. *Biosens. Bioelectron.* **2019**, *145* (May), 111678.
- (26) Rodriguez-Manzano, J.; Moser, N.; Malpartida-Cardenas, K.; Moniri, A.; Fisarova, L.; Pennisi, I.; Boonyasiri, A.; Jauneikaite, E.; Abdolrasouli, A.; Otter, J. A.; Bolt, F.; Davies, F.; Didelot, X.; Holmes, A.; Georgiou, P. Rapid Detection of Mobilized Colistin Resistance Using a Nucleic Acid Based Lab-on-a-Chip Diagnostic System. *Sci. Rep.* **2020**, *10*, 1–9.
- (27) Roskos, K.; Hickerson, A. I.; Lu, H.-W.; Ferguson, T. M.; Shinde, D. N.; Klaue, Y.; Niemz, A. Simple System for Isothermal DNA Amplification Coupled to Lateral Flow Detection. *PLoS One* **2013**, *8* (7), No. e69355.
- (28) Hsieh, K.; Patterson, A. S.; Ferguson, B. S.; Plaxco, K. W.; Soh, H. T. Rapid, Sensitive, and Quantitative Detection of Pathogenic DNA at the Point of Care through Microfluidic Electrochemical Quantitative Loop-Mediated Isothermal Amplification. *Angew. Chem., Int. Ed.* **2012**, *51* (20), 4896–4900.
- (29) Yu, L.-S.; Rodriguez-Manzano, J.; Malpartida-Cardenas, K.; Sewell, T.; Bader, O.; Armstrong-James, D.; Fisher, M. C.; Georgiou, P. Rapid and Sensitive Detection of Azole-Resistant *Aspergillus Fumigatus* by Tandem Repeat Loop-Mediated Isothermal Amplification. *J. Mol. Diagn.* **2019**, *21* (2), 286–295.
- (30) Moser, N.; Rodriguez-Manzano, J.; Lande, T. S.; Georgiou, P. A Scalable ISFET Sensing and Memory Array With Sensor Auto-Calibration for On-Chip Real-Time DNA Detection. *IEEE Trans. Biomed. Circuits Syst.* **2018**, *12*, 390–401.
- (31) Wheeler, D. L.; Chappey, C.; Lash, A. E.; Leipe, D. D.; Madden, T. L.; Schuler, G. D.; Tatusova, T. A.; Rapp, B. A. Database Resources of the National Center for Biotechnology Information. *Nucleic Acids Res.* **2016**, *44* (D1), D7–D19.
- (32) Koyama, T.; Platt, D.; Parida, L. Variant Analysis of SARS-CoV-2 Genomes. *Bull. World Health Organ.* **2020**, *98* (7), 495–504.
- (33) Lu, R.; Zhao, X.; Li, J.; Niu, P.; Yang, B.; Wu, H.; Wang, W.; Song, H.; Huang, B.; Zhu, N.; Bi, Y.; Ma, X.; Zhan, F.; Wang, L.; Hu, T.; Zhou, H.; Hu, Z.; Zhou, W.; Zhao, L.; Chen, J.; Meng, Y.; Wang, J.; Lin, Y.; Yuan, J.; Xie, Z.; Ma, J.; Liu, W. J.; Wang, D.; Xu, W.; Holmes, E. C.; Gao, G. F.; Wu, G.; Chen, W.; Shi, W.; Tan, W. Genomic Characterisation and Epidemiology of 2019 Novel Coronavirus: Implications for Virus Origins and Receptor Binding. *Lancet* **2020**, *395* (10224), 565–574.
- (34) Banoo, S.; Bell, D.; Bossuyt, P.; Herring, A.; Mabey, D.; Poole, F.; Smith, P. G.; Sriram, N.; Wongsrichanalai, C.; Linke, R.; O'Brien, R.; Perkins, M.; Cunningham, J.; Matsoso, P.; Nathanson, C. M.; Olliaro, P.; Peeling, R. W.; Ramsay, A. Evaluation of Diagnostic Tests for Infectious Diseases: General Principles. *Nat. Rev. Microbiol.* **2006**, *4* (S12), 20–32.
- (35) Moser, N.; Lande, T. S.; Toumazou, C.; Georgiou, P. ISFETs in CMOS and Emergent Trends in Instrumentation: A Review. *IEEE Sens. J.* **2016**, *16* (17), 6496–6514.
- (36) Romanov, B. K. Coronavirus Disease COVID-2019. *Saf. Risk Pharmacother.* **2020**, *8* (1), 3–8.
- (37) Broughton, J. P.; Deng, X.; Yu, G.; Fasching, C. L.; Servellita, V.; Singh, J.; Miao, X.; Streithorst, J. A.; Granados, A.; Sotomayor-Gonzalez, A.; Zorn, K.; Gopez, A.; Hsu, E.; Gu, W.; Miller, S.; Pan, C.; Guevara, H.; Wadford, D. A.; Chen, J. S.; Chiu, C. Y. CRISPR-Cas12-Based Detection of SARS-CoV-2. *Nat. Biotechnol.* **2020**, *38*, 870.
- (38) Bi, Q.; Wu, Y.; Mei, S.; Ye, C.; Zou, X.; Zhang, Z.; Liu, X.; Wei, L.; Truelove, S. A.; Zhang, T.; Gao, W.; Cheng, C.; Tang, X.; Wu, X.; Wu, Y.; Sun, B.; Huang, S.; Sun, Y.; Zhang, J.; Ma, T.; Lessler, J.; Feng, T. Epidemiology and Transmission of COVID-19 in 391 Cases and 1286 of Their Close Contacts in Shenzhen, China: A Retrospective Cohort Study. *Lancet Infect. Dis.* **2020**, *20* (8), 911–919.
- (39) Elbe, S.; Buckland-Merrett, G. Data, Disease and Diplomacy: GISAID's Innovative Contribution to Global Health. *Glob. Challenges* **2017**, *1* (1), 33–46.
- (40) Döhla, M.; Boesecke, C.; Schulte, B.; Diegmann, C.; Sib, E.; Richter, E.; Eschbach-Bludau, M.; Aldabbagh, S.; Marx, B.; Eishüßinger, A.-M.; Schmithausen, R. M.; Streeck, H. Rapid Point-of-Care Testing for SARS-CoV-2 in a Community Screening Setting Shows Low Sensitivity. *Public Health* **2020**, *182* (Jan), 170–172.
- (41) Green, K.; Graziadio, S.; Turner, P.; Fanshawe, T.; Allen, J. *Molecular and Antibody Point-of-Care Tests to Support the Screening, Diagnosis and Monitoring of COVID-19*; Oxford COVID-19 Evid. Serv., 2020.
- (42) Carter, L. J.; Garner, L. V.; Smoot, J. W.; Li, Y.; Zhou, Q.; Saveson, C. J.; Sasso, J. M.; Gregg, A. C.; Soares, D. J.; Beskid, T. R.; Jervey, S. R.; Liu, C. Assay Techniques and Test Development for COVID-19 Diagnosis. *ACS Cent. Sci.* **2020**, *6* (5), 591–605.
- (43) Edgar, R. C. MUSCLE: Multiple Sequence Alignment with High Accuracy and High Throughput. *Nucleic Acids Res.* **2004**, *32* (5), 1792–1797.

(44) Kearse, M.; Moir, R.; Wilson, A.; Stones-Havas, S.; Cheung, M.; Sturrock, S.; Buxton, S.; Cooper, A.; Markowitz, S.; Duran, C.; Thierer, T.; Ashton, B.; Meintjes, P.; Drummond, A. Geneious Basic: An Integrated and Extendable Desktop Software Platform for the Organization and Analysis of Sequence Data. *Bioinformatics* **2012**, *28* (12), 1647–1649.

(45) Zadeh, J. N.; Steenberg, C. D.; Bois, J. S.; Wolfe, B. R.; Pierce, M. B.; Khan, A. R.; Dirks, R. M.; Pierce, N. A. NUPACK: Analysis and Design of Nucleic Acid Systems. *J. Comput. Chem.* **2011**, *32* (1), 170–173.

(46) SantaLucia, J.; Hicks, D. The Thermodynamics of DNA Structural Motifs. *Annu. Rev. Biophys. Biomol. Struct.* **2004**, *33* (1), 415–440.

(47) Yu, L.-S.; Rodriguez-Manzano, J.; Moser, N.; Moniri, A.; Malpartida-Cardenas, K.; Miscourides, N.; Sewell, T.; Kochina, T.; Brackin, A.; Rhodes, J.; Holmes, A. H.; Fisher, M. C.; Georgiou, P. Rapid Detection of Azole-Resistant *Aspergillus Fumigatus* in Clinical and Environmental Isolates by Use of a Lab-on-a-Chip Diagnostic System. *J. Clin. Microbiol.* **2020**, *58* (11), 843-20.